AALBORG UNIVERSITY

DENMARK

Hardy space nonlinear controller design for DC microgrid with constant power loads

Rai, Ila; R, Anand; Lashab, Abderezak; Guerrero, Josep M.

Hardy space nonlinear controller design for DC microgrid with constant power loads

Ila Rai [a,*], Anand R [a], Abderezak Lashab [b], Josep M. Guerrero [b]

[a] *Department of Electrical and Electronics Engineering, Amrita School of Engineering, Bengaluru, Amrita Vishwa Vidyapeetham, India*
[b] *Department of Energy Technology, Aalborg University, Aalborg, Denmark*

A B S T R A C T

The increased use of DC microgrid for critical application lead to the necessity of advanced control design for a stable operation of the system. The loads connected to DC microgrid are controlled with power electronic devices and shows the behaviour of constant power load (CPL), which poses a serious challenge to stability as it adds nonlinearity and minimises the effective damping. This paper presents a robust controller design approach based on Hardy Space (H)-infinity control norms to tackle the nonlinearity added by CPL by expanding the region for stability. The design criteria are based on Lyapunov theory of nonlinear systems within the framework of Linear Matrix Inequality (LMI). The necessary and sufficient conditions are obtained in terms of linear matrix inequalities to ensure the transient performance and stability of the system. The LMI equation is solved to maximize the size of the estimated domain of stability. The performance of the proposed controller is verified using simulation in MATLAB/Simulink. The DC microgrid in this paper consists of a solar photovoltaic (PV) unit and a battery as an energy storage system together with loads. The Proposed controller not only ensures the stability of the system but also guarantees the improved transient performance of the closed loop system by expanding the size of the stability region.

1. Introduction

The need for more electricity poses a major challenge to the existing power system. In recent years, renewable energy sources have been rapidly deployed to meet the need for reliable energy and have proved to be the best replacement for conventional energy. The increasing participation of renewable energy sources may lead to complications related to voltage and frequency control including protection issues if directly connected to the utility grid [1]. The so-called microgrid has been designed to overcome these connectivity issues. Microgrids con-nected to renewable energy sources and advanced power electronics devices are utilized to replace the traditional power network by distributed customer driven network to meet the energy demand. Microgrids can be AC or DC. DC microgrids are considered to be a better option due to many advantages compared to the AC ones, such as increased efficiency due to fewer conversion stages, simple integration with energy storage and good compatibility with consumer electronics. In addition, there are no issues with the frequency regulation and reactive power flow linked to the DC bus, which further minimizes the complexity of the control system [2]. The increased participation of

renewable energy sources in DC microgrid has led to the need for advanced control design. The control challenge is to maintain the desired voltage level at the load terminal and manage the uninterrupted power supply while coping with the intermittent nature of renewable energy sources considering variable loads.

DC microgrids are connected to various loads through tightly regulated closed loop-controlled converters to keep the voltage level up to a reference value. These converters exhibit the constant power load behaviour and tend to maintain the load power constant under small variations in the load. The constant power load (CPL) means, the converter's output power will be constant if the system losses are neglected, i.e., when there is a slight increase in the current value, the voltage value will drop to keep the load power constant [3]. The CPL shows negative incremental impedance characteristics as relative rate of change be-tween the voltage and current is negative. The biggest challenge to manage and control the power flow in DC microgrid is the negative incremental impedance effect shown by the CPLs which tends to destabilize the system. The CPLs put a serious threat on the control operation as it minimises the effective damping and destabilises the system. The CPLs are nonlinear in nature where the linear control design

* Corresponding author.
E-mail addresses: rai_ila@blr.amrita.edu (I. Rai), r_anand@blr.amrita.edu (R. Anand), abl@et.aau.dk (A. Lashab), joz@et.aau.dk (J.M. Guerrero).
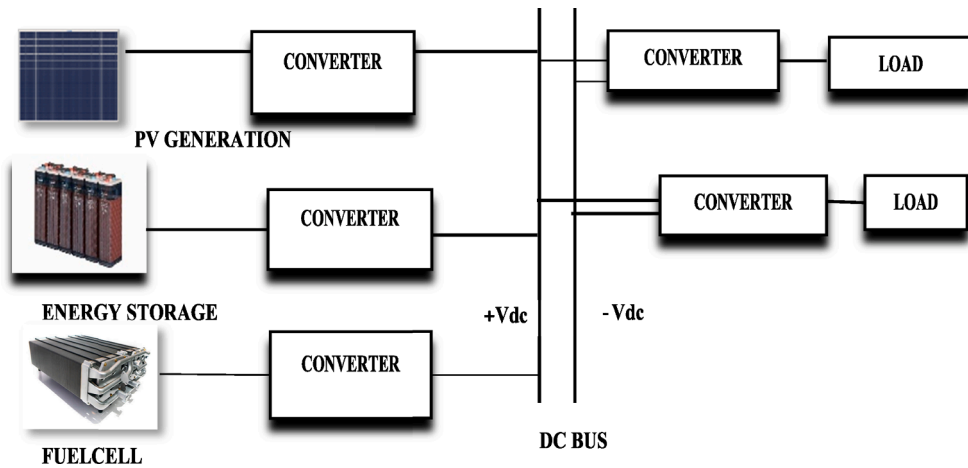
Fig. 1. Block Diagram of DC Microgrid.

may not give the satisfactory results as they provide only local stability [4]. The nonlinear nature of CPLs in DC microgrid requires the use of nonlinear control approaches to moderate the unwanted effects of CPLs as well as to evaluate the requirements for stability.

Several control approaches dealing with nonlinearity exist to minimize the instability and damaging effect of the CPLs [5,6]. In [7], a model predictive control method is proposed considering the nonlinearity of the model. This method puts a challenge in practical implementation because of its computational requirements. Sliding mode control provides robust stability ensurance but fails to control the chattering issue. Moreover, the use of equivalent series resistance (ESR) degrades the ripple filtering effect with increased output impedance [8]. One more approach for nonlinear control of DC microgrids with CPLs is passivity-based control [9]. This method requires a very accurate model and also a variation in the operating point may lead to a tracking error [10,11]. The backstepping algorithm is not directly dealing with the regulation of the output voltage and may cause a steady state tracking error. Usually, unknown inputs and external disturbances affect nonlinear systems, making it difficult to ensure the stability assessment and control design. To cope with these issues T-S fuzzy models with quadratic Lyapunov functions have been developed [12]. However, fuzzy controller involves a lot of IF-THEN rules and also the defuzzification procedure is very time-consuming and hard to implement with simple hardware. Existing work on control of DC microgrid have many limitations in spite of substantial research. These methods are unable to provide a systematic control approach and stability analysis for general topology as the approaches are specific to a particular application, each [13–17].

The available control approaches are unable to answer the uncertainty caused by the large signal deviation from the operating point due to the increased complexity. Some control approaches may provide only local stability while global stability analysis is required to minimise the negative effects of large signal deviations in the system. In order to determine the stability conditions, it is important to estimate the domain of attraction around the possible operating points. [18,19]. The domain of attraction (DA) is a collection of original states for which all trajec-tories begin to converge to the equilibrium point for a specified local asymptotically stable equilibrium point. By estimating the DA, system stability and security margin can be directly predicted in relation to a specified original state [20,21]. The nonlinear H-infinity control theory offers a feasible way to design a robust non-linear controller that in-volves the estimation of DA. However, the first order of nonlinear dif-ferential inequality called Hamilton-Jacobi-Isaac's (HJI) inequality must be resolved to use the outcomes of this theory. The primary drawback is the lack of a systematic approach to solve the HJI's inequality for using the outcomes of nonlinear H-infinity control theory.

In order to overcome the limitations of HJI's inequality approach, a method based on the nonlinear H-infinity control problem is solved based on linear matrix inequality approach [22]. The resulting technique provides not only a solution to the issue, but also a valid area of estimation. In [23], the control problem is formulated and solved as an optimization problem. This technique has an advantage over the clas-sical method that it gives an appropriate method for problems related to multivariate structures. In [24,25], the nonlinear H-infinity control issue is solved on the basis of Lyapunov function approach combining the understanding of linear matrix inequality. The design guarantees the stability and performance of the controller even if there is a variation in presumed plant and actual plant.

The literature review indicates that achieving suitable transient performance including stability, is very challenging as the current nonlinear approaches are too complex. Furthermore, the existing control methods may not improve the overshoot performance and settling time all together [26–31]. Therefore, in addition to the stability issues, additional efforts are required to optimally and effectively mitigate the effect of the CPLs.

In this paper, a controller design satisfying H-infinity norms is presented to improve the stability and performance of the DC microgrid with multiple CPLs. The proposed approach not only provides stability for the system in the defined stability region but also maximises the domain of stability while improving the robustness of the system. In this paper, new adequate local requirements for the controller are developed with regard to linear matrix inequalities (LMIs), which can be easily solved through convex programming methods. The LMIs, thus calculated, ensure the improved transient performance and keep the settling time minimum for the closed-loop DC microgrid system. At last, the validity evaluation is done in MATLAB/Simulink. The results not only indicate the improved transient performance, but also the improved overshoot and settling time during disturbance.

This Paper is arranged as follows: In Section 2 the DC microgrid is modeled and the problem is formulated. The proposed architecture for stability and control is discussed in Section 3. In Section 4, a controller design is developed based on proposed architecture and the design is applied to the DC microgrid model. Simulation validation is given in Section 5 to highlight the benefits of the method. The last Section concludes the presented work.

2. DC microgrid modelling and problem formulation

The space state model of DC microgrid combining all sources and CPLs as well as all buses connected to it can be presented in the form:
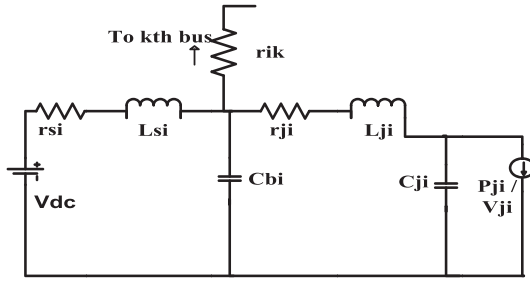
$$\dot{x} = Ax + Bu + f(x) \tag{1}$$
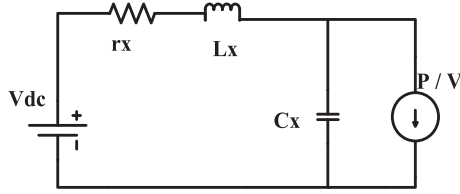
Fig. 2. The ith Bus diagram of DC Microgrid.

Fig. 3. Simplified diagram of DC Microgrid with CPL.

Fig. 4. Phase portrait of (x1) based on circuit parameters given in Table 1.

$$Z = Cx \tag{2}$$

where x and Z are the state vector and output vector, respectively. The matrix A is state or system matrix of $n \times n$ dimension, B is the input matrix of $n \times m$ dimension and C is the output matrix of $l \times n$ dimension.

The vector $x \in R^n$ where R represents the set of real numbers, and u is the control input matrix.

The nonlinear function $f(x)$ and vector x are specified as:

$$f(x) = \left[-\frac{P_{11}}{v_{11}} \cdots \cdots -\frac{P_{1n}}{v_{1n}} \right] \tag{3}$$

$$x = \left[i_x^T, v_x^T \right] \tag{4}$$

Here i_x and $v_x \in R^{2n}$. i_x presents all source and load currents while v_x presents all bus and load voltages respectively, while $P = [P_{11}, \cdots \cdots P_{1n}]^T$ and $v = [v_{11}, \cdots \cdots v_{1n}]^T$ are defined as constant load power and voltage.

The loads in DC microgrid behave as constant power load and acts as current sink as shown in Fig. 2. The value of the current is measured by the CPL power divided by its voltage. These CPLs are nonlinear and hence exhibit a negative incremental impedance v-i characteristics which may cause instability in the system.

The dynamic equations for the DC microgrid bus model in Fig. 3 are given by

$$\dot{x}_1 = -\frac{r_x}{L_x}x_1 - \frac{1}{L_x}x_2 + \frac{1}{L_x}V_{dc} \tag{5}$$

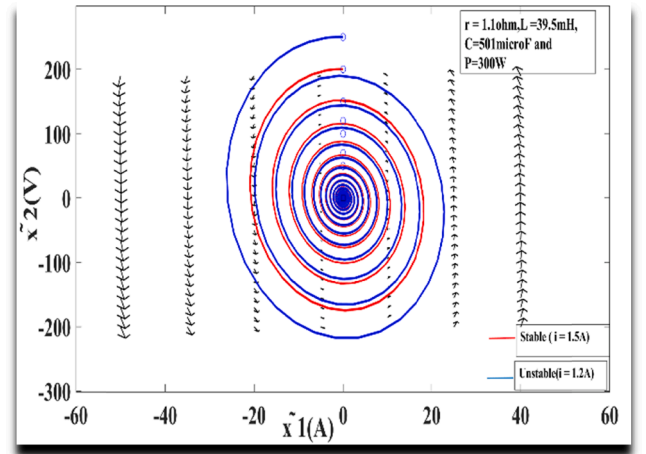$$\dot{x}_2 = \frac{1}{C_x}x_1 - \frac{1}{C_x}f(x_2) \tag{6}$$

where x_1 and x_2 are the inductor current and capacitor voltage respectively, while $f(x_2) = P/(x_2)$ and represents CPL. Here r_x represents the source resistance as shown in Fig. 3.

The Equilibrium Point is calculated as:

$$V_{eq} = \frac{V_{dc} \pm \sqrt{(V_{dc}^2 - 4Pr_x)}}{2} \tag{7}$$

$$I_{leq} = P/V_{eq} \tag{8}$$

The equilibrium points of the system will be real and positive if the value of Pr_x is small. The equilibrium point is complex if the value of Pr_x is larger than V_{dc}^2. In this case, there is no physically feasible point of operation. Hence, the following condition must be satisfied to avoid complex equilibrium points:

$$r_x < \frac{V_{dc}^2}{4P} \tag{9.a}$$

This restriction imposes an upper limit on the source resistance which depends only on the amount of power supplied by the source and operating voltage. The violation of the condition given by equation (9.a) leads to instability of the system.

A safety measure has to be taken to maintain a stable operation. The equation (9.a) can be rewritten after applying a safety factor of 2 as:

$$r_x < \frac{V_{dc}^2}{8P} \quad \text{or} \quad P < \frac{V_{dc}^2}{8r_x} \tag{9.b}$$

If the source resistance is 5% of the load resistance, then equation (9.b) is expressed as:

$$P < \frac{V_{dc}^2}{8*0.05r_x} < 2.5*P_{rated} \tag{9.c}$$

The condition given in equation (9.c) puts a limit on the system voltage, CPL and source resistance; however, equilibrium points may not exist during large transients because of these constraints. This condition just supports the local stability and does not explain the global stability of the system [12]. Local stability condition may not ensure the safe operation of the system because of the nonlinearity added by the function $f(x)$ in the model. These nonlinearities cannot be neglected for the stability analysis during large signal deviation. In addition, the condition gives no information about the DA for the operating point of the DC link voltage.

The DA of a dynamic system is a set of state-space whose respective trajectories converge to an asymptotically stable equilibrium point.

The DA of the equilibrium point $x = 0$, is given by:

$$DA(0) = \left\{ x_0 \in R^n : \lim_{t \to \infty} x(t, x_0) \to 0 \right\} \tag{10.a}$$

In order to ensure a stable dynamic behaviour of the nonlinear system in the State Space Domain, the DA should be assessed. The DA explains how a small disturbance in the system can push the system to the unstable region. To understand this fact a small perturbation in state vector is done around its operating point. The system presented by (5), (6) can be rewritten as:

$$\dot{\tilde{x}}_1 = -\frac{r_x}{L_x}\tilde{x}_1 - \frac{1}{L_x}\tilde{x}_2 \tag{10.b}$$

$$\dot{\tilde{x}}_2 = \frac{1}{C_x}x_1 + \frac{P}{C_x(x_2)}f1(x_2) \tag{10.c}$$

The power P is assumed to be constant. $\dot{x}_1, \dot{x}_2$ present the small perturbation in inductor current and capacitor visualise the problem, the circuit parameters shown in Fig. 3 are considered as $R_x = 1.1$ Ω, $L_x = 39.5$ mH, $C_x = 501$ μF, $V_{dc} = 200$ V, $P = 300$ W. The V_{eq} and I_{eq} are calculated using (7) and (8) and are equal to 198.336 V, 1.51 A respectively.

The current value changes from 1.5 A to 1.2 A. The response of the system is checked and drawn in MATLAB for both the current values. The equilibrium point is said to be asymptotically stable only if the trajectories initiated at the set point will converge to the domain of attraction. It can be observed from the Fig. 4 that the trajectory for current value 1.2A is not converging to the domain of attraction. The system response indicates that any small disturbance on the voltage or current can push the system to the unstable region even though the operating point is stable. The assessment of DA can also explain the impact of different parameters on the stability of the system. The estimation of the DA can be useful for increasing the robustness of the system. Hence, the computation of the DA related to system parameters is of great significance for real-world applications.

3. Proposed architecture for control and stability

A DC microgrid's stability assessment is essential because the system equilibrium depends on uncertain CPLs and changes over time in actual applications. The change in CPL may cause instability in the system. To overcome the computational disadvantages of earlier technique, the state equation is approached in a different way in this paper

The nonlinear system considered in (1) is written in a general form as:

$$\dot{x} = Ax + f(x) \tag{11}$$

Here $x \in R^n$ is the state of the system, A is $n \times n$ constant matrix defining state vector and $f(x)$ represents the nonlinear function of the system.

The quadratic Lyapunov function $V(x)$ is applied to create a robust stability for the given system and also used to estimate the suitable stability region. The function $V(x)$ is a valid Lyapunov function assuming M is a positive definite symmetric matrix of $n \times n$ dimension. The system presented by (7) is asymptotically stable $\left(\lim_{t \to \infty} x(t) = 0, \forall x_0 \neq 0 \right)$ if there exists a quadratic Lyapunov function $V(x) = x^T M x$ such that $V(x) = 0$ and $\dot{V}(x) < 0$, where the DA or stability region of the equilibrium can be defined as:

$$f(.,.) = \{x \in R^n : V(x) = \gamma, \gamma > 0\} \tag{12}$$

For the given system here, if the inequality $\dot{V}(x) = (gradV)\{Ax + f(t,x)\}\langle 0$ and $x \neq 0$ is valid then the system is stable in the domain of attraction of $f(.,.)$.

The nonlinear function $f(x)$ given in (11) is assumed to be uncertain and in the domains of continuity satisfies the given quadratic inequality:

$$f^t(x)f(x) \leq \alpha^2 x^T H^T H x \tag{13}$$

The constraint given in (9) is equivalent to the quadratic inequality shown as:

$$\begin{bmatrix} x \\ f \end{bmatrix}^T \begin{bmatrix} -\alpha^2 H^T H & 0 \\ 0 & I \end{bmatrix} \begin{bmatrix} x \\ f \end{bmatrix} \leq 0 \tag{14}$$

where $\alpha > 0$ is the bonding parameter which assesses the robustness for the system. H is an $m \times n$ constant matrix. The system with a large value of α shows more robustness towards the nonlinear disturbances. The inequality specified in (13) outlines a class of piecewise continuous function for any given H and is defined as:

$$H_\infty = \left\{ f : R^{n+1} \to R^n \middle| f^T f \leq \alpha^2 x^T H^T H x \ in \ the \ domains \ of \ continuity \right\} \tag{15}$$

Here H_∞ is Hardy space matrix-valued function, which represents a maximum gain in any direction. The closed loop effect of the perturbation can be minimised with the help of H_∞ method and will be evaluated in terms of stability. The objective of this paper is to create stability around the operating point. The nonlinear system specified by (1) is robustly stable with degree α if the equilibrium is globally asymptotically stable for all $f(x) \in H_\infty$.

To check the stability of the system, computation of $\dot{V}(x)$ is required, which is given by:

$$\dot{V}(x) = x^T(A^T M + MA)x + f^T M x + x^T M f \tag{16}$$

For system stability, $\dot{V}(x)$ should be less than zero. This happens if and only if

$$x^T(A^T + MA)x + f^T M x + x^T M f < 0 \tag{17}$$

This condition is not convex in M, but by a simple change of variables and using S-procedure, an equivalent condition can be obtained that can be presented as an LMI.

Thus, necessary and sufficient conditions for the existence of quadratic Lyapunov function can be expressed as LMI if the condition (14) satisfies:

$$M > 0$$

$$\begin{bmatrix} AM + YM^T + \tau\alpha^2 H^T H & I \\ I & -I \end{bmatrix} < 0 \tag{18}$$

where τ is the s-procedure constant and is always greater than zero.

If $\alpha^2 = \frac{1}{\gamma}$ and $M = \tau Y$, (18) can be rewritten using Schur's compliment formula as:

$$Y > 0$$

$$\begin{bmatrix} AY + YA^T & I & YH^T \\ I & -I & 0 \\ HY & 0 & -\gamma I \end{bmatrix} < 0 \tag{19}$$

To establish robust stability for a large class of H_∞, the matrix is selected in such a manner so that it can maximise the constraint α and this could be achieved by solving LMI problem in Y, where γ is given below:

Minimize γ
Subject to Y > 0

$$\begin{bmatrix} AY + YA^T & I & YH^T \\ I & -I & 0 \\ HY & 0 & -\gamma I \end{bmatrix} < 0 \tag{20}$$

The system (11) can be stabilized if and only if there exists M > 0 and Y such that the LMI (20) holds. If this LMI is feasible, the quadratic function $V(x) = x^T M x$ will prove the stability of the system (11) with a state-feedback $u = YM^{-1}x$. The feasibility of the LMI condition confirms that the system (11) is robustly stable with degree α.

4. Controller design with Hardy space of matrix valued function

4.1. Controller design

The design of the controller is very important to provide a proper feedback to stabilize the overall system. The DA can be increased using the proper choice of feedback to maximise the tolerance to any uncertain nonlinear disturbance. Energy storage is used to reduce the transients and minimise the fault in DC microgrid.

The proposed controller is designed to increase the domain of

attraction and to optimally modify the energy storage usage.

The term u given in (1) is a control input and expressed as:

$$u(x) = Kx \tag{21}$$

Here K is a constant gains matrix of $n \times m$ size.

The closed-loop system equation after applying the feedback is written as:

$$\dot{x} = \hat{A}x + f(.,.) \tag{22}$$

where $\hat{A} = A + BK$ is defined as the closed loop system matrix.

The aim of implementing the feedback is not only to stabilize the system, but also to boost the uncertainty bound α. Feedback control can stabilize the system (7) robustly if the closed-loop system is also robustly stable with degree α.

Using Lyapunov function $V(x)$ and taking its derivative $\dot{V}(x)$, the problem (20) can be formulated as:

Minimise γ
Subject to $Y > 0$

$$\begin{bmatrix} AY + YA^T + BKY + YK^TB^T & I & YH^T \\ I & -I & 0 \\ HY & 0 & -\gamma L \end{bmatrix} < 0 \tag{23}$$

But the equation formulated above may not be in the form of LMI in Y and K. The Equation can be converted to LMI problem by changing the variable as:

$$KY = L \text{ or } K = LY^{-1} \tag{24}$$

To ensure the proper value of $\overline{\alpha}$, the size of the gain matrix should be limited to make the system practical.

The system is set as:

$$L^T L < K_l I, K_{l>0}$$

$$Y^{-1} < K_y I, K_y > 0 \tag{25}$$

where K_y, K_l are the bounding norm for the gain matrix K

To fix the proper value of $\overline{\alpha}$

$$\gamma - \frac{1}{\overline{\alpha}^2} < 0 \tag{26}$$

Combining all the constraints, the final optimization problem is modified as:

Minimise $\gamma + K_l + K_y$
Subject to $Y > 0$

$$\begin{bmatrix} AY + YA^T + BL + L^TB^T & B & YH^T \\ B^T & -I & 0 \\ HY & 0 & -\gamma L \end{bmatrix} < 0$$

$$\gamma - \frac{1}{\overline{\alpha}^2} < 0$$

$$\begin{bmatrix} -K_l I & L^T \\ L & -I \end{bmatrix} < 0$$

$$\begin{bmatrix} Y & I \\ I & K_y I \end{bmatrix} > 0 \tag{27}$$

The system will be robustly stabilizable with a degree $\overline{\alpha}$ by control law if the problem (27) is feasible.

Algorithm for H∞ controller using LMIs

Assume that system matrices A, B, C, D are given
1: Find L, Y ∈ Sn that satisfy (16).
2: Calculate the value of M
3: Solve (21) to get the controller system matrix K.

---

*Sn = The positive definite cone of symmetric matrices

4.2. Proposed framework for DC microgrid with multiple CPL

In this paper, we consider a DC microgrid with multiple CPLs as shown in Fig. 1.The proposed method is applied to compute the domain of attraction for multiple CPLs, while an energy storage connected to the DC microgrid. Based on (5), the dynamic model of the ith bus in the system shown in Fig. 2 has the following form:

$$\dot{x}_i = A_i x_i + b_i f_i + A_{is} x_s \tag{28}$$

where $i \in I_n \triangleq \{1, 2, \cdots\cdots n\}$ and $s \triangleq n+1$ represents the source. $x_s = [x_{1,s}, x_{2,s}]^T = [i_{L,s} v_{C,s}]^T$ and $x_i = [x_{1,j} x_{2,j}]^T = [i_{L,i} v_{C,i}]^T$ represents the source and CPLs state vectors, respectively.

The system matrices are written as:

$$A_i = \begin{bmatrix} -\dfrac{r_i}{x_i} & \dfrac{-1}{L_i} \\ \dfrac{1}{C_i} & 0 \end{bmatrix},$$

$$b_i = \begin{bmatrix} 0 \\ \dfrac{1}{C_i} \end{bmatrix},$$

$$A_{is} = \begin{bmatrix} 0 & \dfrac{1}{L_i} \\ 0 & 0 \end{bmatrix},$$

$$b_{bat} = \begin{bmatrix} 0 \\ \dfrac{-1}{C_s} \end{bmatrix}$$

Referring to (5), the source subsystem can be written as:

$$\dot{x}_s = A_s x_s + b_s V_s + b_{bat} i_{bat} + \sum_{i=1}^{n} A_{cn} x_i \tag{29}$$

where

$$A_s = \begin{bmatrix} -\dfrac{r_s}{x_s} & \dfrac{-1}{L_s} \\ \dfrac{1}{C_s} & 0 \end{bmatrix},$$

$$b_s = \begin{bmatrix} \dfrac{1}{L_s} \\ 0 \end{bmatrix},$$

$$A_{is} = \begin{bmatrix} 0 & 0 \\ \dfrac{-1}{C_s} & 0 \end{bmatrix},$$

$$b_{bat} = \begin{bmatrix} 0 \\ \dfrac{-1}{C_s} \end{bmatrix}$$
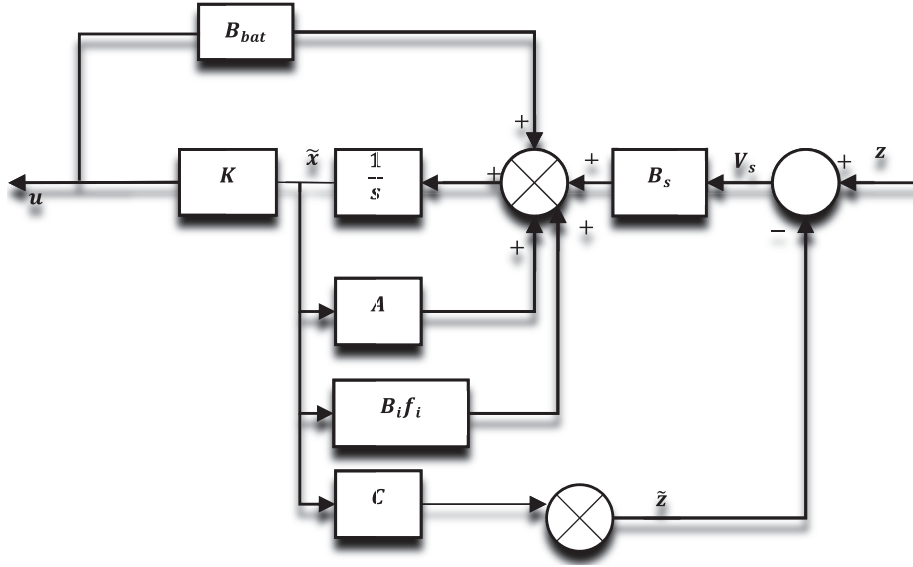
Assuming a coordinate change about an operating point and considering the energy storage current i_{bat} as a control input, the dynamic model of the DC microgrid is rewritten as:

$$\dot{\tilde{x}} = A\tilde{x} + B_i f_i + B_{bat} \tilde{i}_{bat} + B_s V_s \tag{30}$$

Here, the state variable x is defined as:

$$x = (x1, x2, \cdots..xn)^T, A = \begin{bmatrix} A_1 & . & . & . \\ . & A_2 & . & . \\ . & . & A_n & . \\ A_{cn} & . & A_{cn} & A_s \end{bmatrix},$$

Fig. 5. Block diagram of H_∞ Controller.

$$B_i = \begin{bmatrix} b_1 & . & . & . \\ . & b_2 & . & . \\ . & . & . & . \\ . & . & . & b_n \\ 0 & 0 & 0 & 0 \end{bmatrix}, B_{bat} = \begin{bmatrix} 0 \\ 0 \\ b_{bat} \end{bmatrix}, B_s = \begin{bmatrix} 0 \\ 0 \\ b_s \end{bmatrix}$$

and the nonlinear function is given as $f_x = (f_1, \cdots .f_n)^T$

Where

$$f_i\left(\tilde{x}_i\right) = \frac{\tilde{x}_i}{x_{i0}\left(\tilde{x}_i + x_{i0}\right)}, i \in I_n$$

where x_i is used to represent the state of the ith CPL and x_{i0} is the operating point for that corresponding state. It is assumed that the nonlinear term $f_i\left(x_i\right)$ should satisfy a quadratic bond given as in (30).

The objective is to apply a feedback to compute the DA with multiple CPLs while increasing the bounding parameter α. The block diagram for H_∞ Controller is shown in Fig. 5.

4.3. Stability analysis

Multiple constant power loads are susceptible to the interaction between the parallel filters. These interaction including negative impedance of the CPLs will increase the negative damped oscillations. The stability criteria discussed above are applicable to multiple load systems. The asymptotic stability of the system is proved if the LMI (27) is feasible. In this case, it is possible to evaluate Y verifying (27), so that the Lyapunov function $V(x) = x^T M x$ is completely realized.

The existance of Y given in (27) depends on two conditions:

(i) Stae matrix A_i is hurwitz
(ii) $A_i = \sum_{i=1}^{r} A_i$ is Hurwitz

If A_i is positive definite, nonlinear function $f(x) \to \infty$ as $v \to \infty$ and norm of $K < 1$ then for all currents and voltages each solution tends to the set of equilibrium points while $t \to \infty$.

This is the condition that must be satisfied by the multiple load system in order to have a non-oscillatory response during large disturbances. The state matrix A_i can be calculated directly from the nonlinear model by setting a constant limit value (min., max.) for each of the n nonlinearities. These limits value specify a domain where the stability
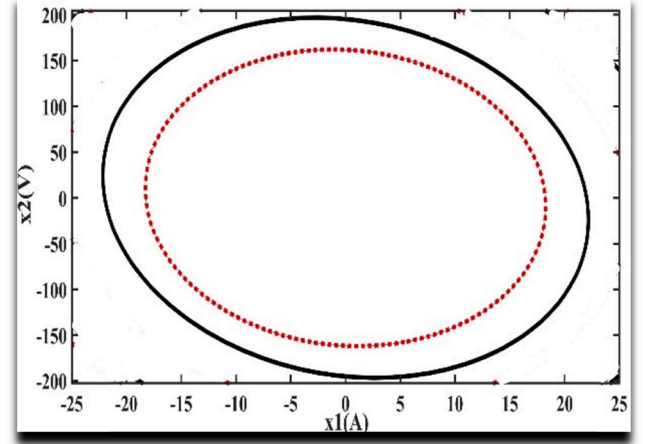

Fig. 6. Comparison of Domain of attraction with and without the proposed controller (proposed approach is shown by black line and DA without control is shown by dashed red line).

analysis is valid. However, the main downside to this approach is that with the number of nonlinearities, complexity grows rapidly. Nonetheless, if there are q nonlinearities, 2q matrices can be handled. The proposed design only checks the stability for an extreme case for A_{imax}, instead. It is observed that A_{imax}'s Hurwitz stability guarantees the stability of all matrices in A_i by lower bounding the smallest eigen value. When analysing the system matrix structure, it is viewed that lower bound occurs only when the upper bound is the largest possible parameter uncertainty f(x). To compute the DA assume $x \in R^n$ and there exists a diagonal matrices $H \geq 0$ such that it satisfies the condition given in (27). If problem (27) is feasible and $K \leq 1$ then the estimated DA can be computed as a larger set given as:

$$\Omega(r) = \left\{ x \in R^n \big| V(x) = x^T M x \leq r \right\} \tag{31}$$

The benefit of the proposed algorithm for calculating the DA is that the LMIs do not exponentially increase with the increase in the number of CPLs. A comparison of DAs with and without control is given in Fig. 6. It is observed that the DA can be increased by minimising the norm of K while increasing the robustness index ∝ .

Table 1
System Parameters for Simulation with Multiple CPLs.

Vdc = 200 V	R1 = 0.8 Ω	R2 = 0.42 Ω
Rs = 0.4 Ω	L1 = 40 mH	L2 = 19.5 mH
Ls = 17.3 mH	C1 = 1 mF	C2 = 1.05
Cs = 1.05 mF	P1 = 900 W	P2 = 600 W

5. Simulation validation

To assess the validity of the suggested approach, simulations were conducted on MATLAB/Simulink. The robustness index calculated by equation (23) is given as $\alpha_n = .0224$. The proposed controller is simulated for multiple CPLs based on the parameters given in Table −1. The value of the controller gain matrix by solving equation (27) is achieved as follows: K = [0.8056–0.0205 0.0 0.0 0.9520 0.0845] and value of robustness index is calculated as $\alpha = 0.099$. The improved value of the robustness index shows that the size of the DA is improved with the above proposed controller design. The state variables were guaranteed to be inside the LMI region and provide a feasible solution while optimizing the gain matrix value.

The case study is done based on the parameters given in Table 1. The PV system has a maximum power rating of 10 KW with solar irradiance of 1000 W/m^2. The operating temperature is 298 K while the nominal dc-bus voltage is considered to be 200 V. The energy storage system connected in parallel has a nominal voltage of 48 V dc and 150 Ah capacity. The results are evaluated in different operating conditions. The robustness index calculated using this method is $\propto = 0.099 > \propto_n$. The increased value of robustness index will lead to increased size of stability region.

Case I – Under changing load conditions with multiple CPLs: The PV system operates at STC irradiance and temperature. At t = 0.5 sec the load demand increases from 600 W to 900 W. A conventional PI controller as shown in Fig. 7 is used for comparative purposes to assist in evaluating the proposed controller performance. Initially, the PI controller is simulated under varying load condition. Then, the proposed control algorithm is used for simulation under the same condition and compared with the PI controller in terms of performance. The system responses of both the controller are shown in Figs. 8–10. A major change in load can cause a large disturbance to the output voltage.

Fig. 8 shows the simulation result of bus voltage response under varying load demand using the PI and proposed controller. At t = 0.5 s the bus voltage gets disturbed because of the increase in load demand. The diagram shows that the system can achieve stability even if the CPL variations are significant where the output voltage tracks the reference voltage at 200 V accurately using the proposed controller design. The
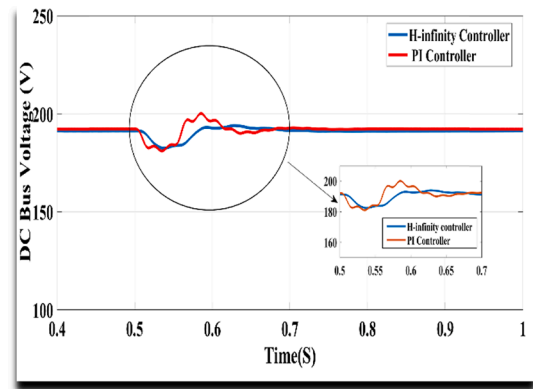

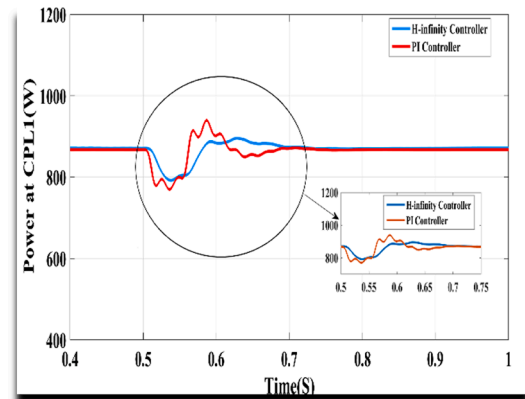**Fig. 8.** DC Bus voltage under changing load demand.

Fig. 9. Power at CPL1 under changing load demand.

system stabilizes fast compared to PI controller. Though, the PI controller is able to stabilise the bus voltage, transient responses still have scope for improvement as shown in the diagram. The overshoot is larger compared to the proposed controller and takes more time to converge. The comparison shows that the proposed controller is able to offer better transient performance while minimising the overshoot and settling time.

Figs. 9 and 10 show the power at constant power load1 (CPL1) and constant power load2 (CPL2) under varying load demand. The
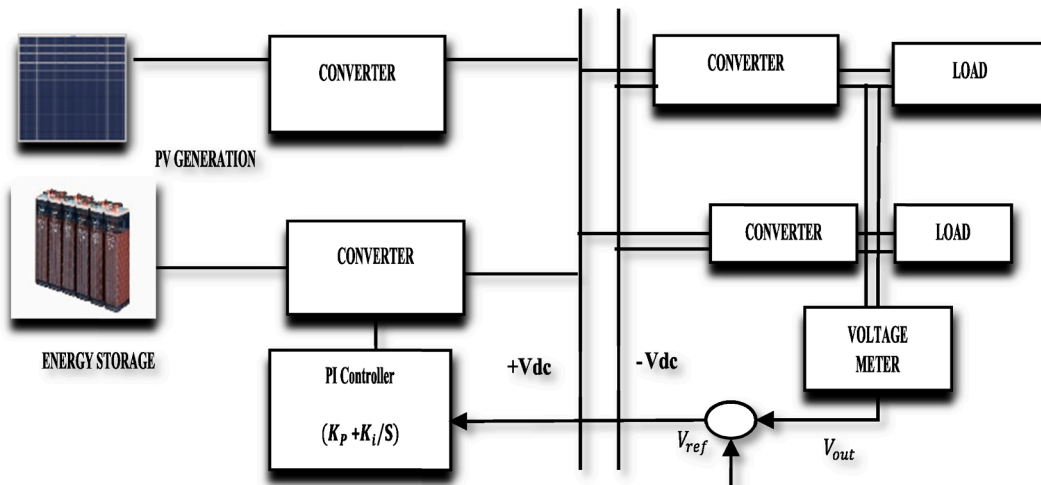

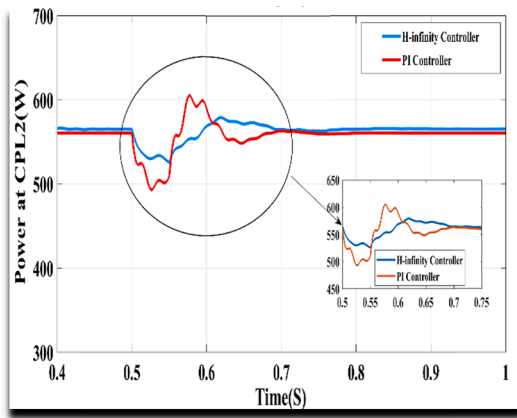**Fig. 7.** Schematic diagram of PI controller.
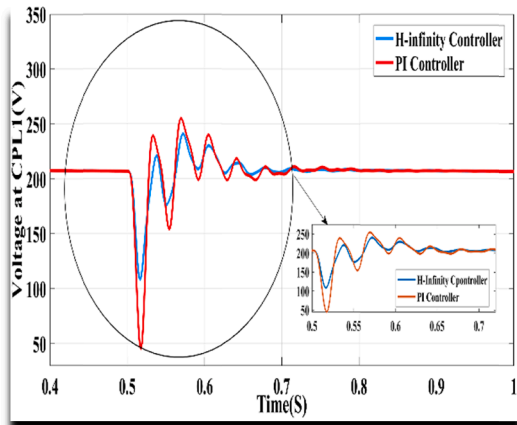
Fig. 10. Power at CPL2 under changing load demand.

Fig. 11. Voltage at CPL1(V).

Fig. 12. Voltage at CPL2(V).

Fig. 13. Current at CPL1, IL1(A).
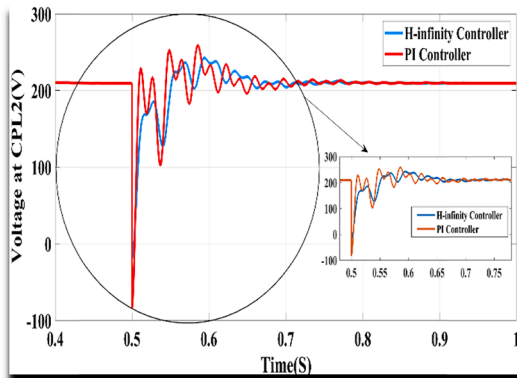

Fig. 14. Current, IL2(A).

Fig. 15. DC Bus Voltage under fault condition.

simulation result shows that the proposed controller offers better power balance during load variation compared to the PI controller. The percentage overshoot and settling time both are less compared to the PI controller.

Case II – Under Fault condition: A fault for 0.2 s is introduced at the DC link to evaluate the performance of the proposed controller. The system is working at the nominal parameters as given in Table 1. The fault will force the system to be in an unstable state if not managed. The voltage and current at CPL1 and CPL2 are shown in Figs. 11–14. Fig. 15 shows the bus voltage variation under fault.

The simulation results show the changes in load current and voltage
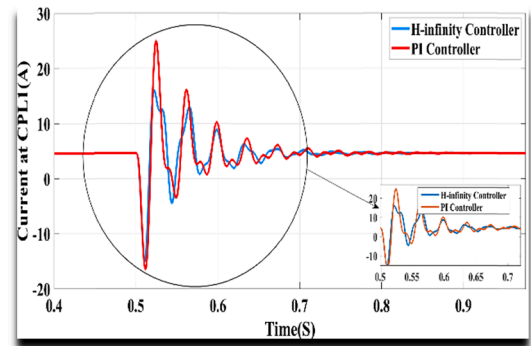
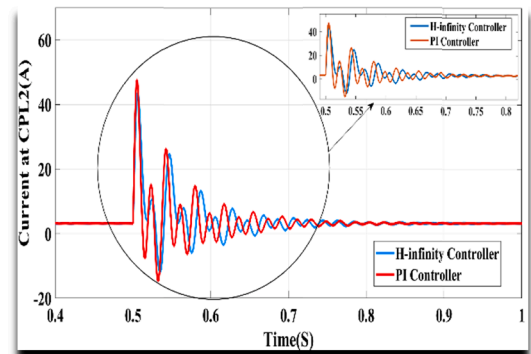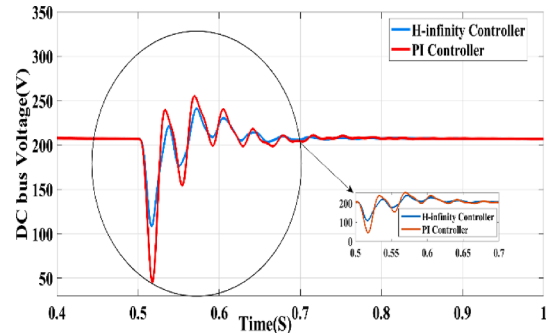during the fault condition. The proposed controller can be triggered by actively charging or discharging the battery during the fault condition. Figs. 13 and 14 show that, the controller is able to regulate the current within a few milliseconds with a smaller overshoot after the occurrence of the disturbance. Fig. 15 shows that the bus voltage can be stabilized by both algorithms. The conventional PI control, however, causes a large transient response and takes longer time to converge than the controller proposed.

It can be observed from the system's response that the designed

Table 2
Time Response for the different Approaches for DC microgrid control.

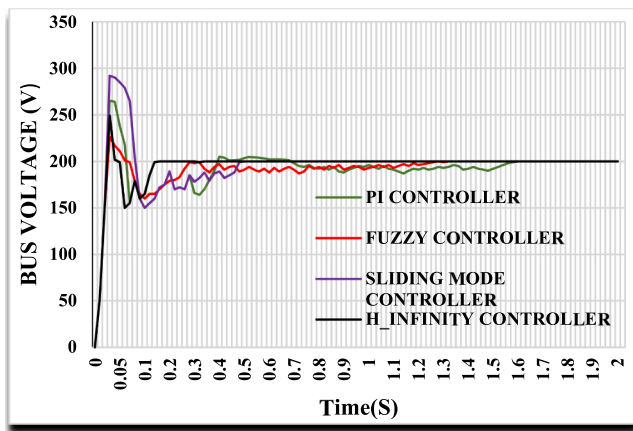| Controller Design Approach	Settling time (s)	% overshoot	% Steady state error
PI	1.6091	0.326	0.9231
Fuzzy PID	1.3609	0.132	0.2325
Sliding Mode	0.5	0.46	–
Proposed design	0.14	0.245	0.021

Fig. 16. DC Bus Voltage Transient Response.

controller helps the microgrid to recover these disturbances quickly. The comparison of settling time, overshoot and steady state error for different approaches are given in Table 2. It is observed that the performance of the proposed controller is better than that of PI, Fuzzy PID, Sliding mode controller in terms of maximum overshooting, settling time, and steady state errors.

The transient response of the various approaches, including the proposed approach, has been compared in Fig. 16. As shown in this figure, for PI, fuzzy PID, sliding mode approach, the settling times are 1.6091, 1.3609, 0.5, respectively. The corresponding observed value for the proposed approach is equal to 0.14. Similarly, the percentage overshoots and steady state error are also compared. The value of percentage steady state error for proposed controller is 0.021, while for PI and Fuzzy PID controller the corresponding values are 0.9231 and 0.2325. Compared to other approach, the settling time and steady state error are minimum for proposed approach.

The percentage overshoot values for PI, Fuzzy PID, Sliding mode and proposed controller are 0.326, 0.132, 0.46, 0.245, respectively. The proposed controller shows less overshoot compared to PI and Sliding mode controller. It can therefore be concluded that the proposed approach has improved performance compared to the PI, fuzzy PID and sliding mode control approach.

6. Conclusion

In this paper, a new method for controller design based on H-infinity norms is proposed. The design of the controller includes the nonlinearity imposed by CPLs. To assess the validity of the suggested approach simulations conducted on MATLAB with LMI solver. The case study is done based on parameters given in Table 1. The performance of the proposed controller was evaluated by testing it for two conditions: (i) under changing load condition (ii) under fault condition. The large variations in load or fault over a long period of time may lead to voltage instability within the network. The proposed controller not only stabilizes the system fast but also improves the transient response under these conditions. The performance of the proposed controller is compared in terms of steady state error, percentage overshoot and settling time with PI, Fuzzy PID, Sliding mode controller. The comparison shows that the transient and steady state response are improved compared to other approaches. The proposed approach does not require the time derivatives of states. This makes the approach more robust against noises compared to other control design. Since this approach utilizes the nonlinear function, it is more robust against uncertainties compared to other linear approaches. Besides, the proposed approach provides the global stabilization by increasing the DA. The formulation demonstrates the feedback gain calculation method used to achieve the necessary robustness index with an optimum value of norm of gain. The size of the

DA can be enlarged at the required level by enhancing the robustness index which will improve the system control. The increased value of robustness index will lead to increased size of DA or stability region. The outcomes of the simulation show that the closed-loop performance of proposed controller with CPLs has improved compared to the conventional PI controller. The result shows that the DA of the closed-loop DC MG scheme with CPLs has improved considerably. The proposed controller adjusts the injecting power while minimising it and applied it through the energy storage to the nonlinear DC microgrid system and hence improving the performance of the system. The proposed controller not only mitigates the faults or disturbances in dc bus voltage but also tackles the issues of load variations in CPLs. The main benefit of the proposed method is a decreased level of complexity with an increased number of CPLs. Therefore, with less complexity, the performance of the DC microgrid with multiple CPLs can be improved.

Declaration of Competing Interest

The authors declare that they have no known competing financial interests or personal relationships that could have appeared to influence the work reported in this paper.

References

[1] Planas Estefanía, Andreu Jon, Gárate JoséIgnacio, de Alegría Iñigo Martínez, barra EdortaI. AC and DC technology in microgrids: A review. Renew Sustain Energy Rev 2015;43:726–49.

[2] Dragičević Tomislav, Lu Xiaonan, Vasquez Juan C, Guerrero Josep M. DC Microgrids—Part I: A Review of Control Strategies and Stabilization Techniques. IEEE Trans Power Electron 2016;31(7).

[3] Emadi A, Khaligh A, Rivetta CH, Williamson GA. Constant power loads and negative impedance instability in automotive systems: Definition, modeling, stability, and control of power electronic converters and motor drives. IEEE Trans Veh Technol 2006;55(4):1112–25.

[4] Wu M, Lu DD-C. A novel stabilization method of LC input filter with constant power loads without load performance compromise in DC microgrids. IEEE Trans Ind Electron 2015;62(7):4552–62.

[5] Liu Jianzhe, Zhang Wei, Rizzoni Giorgio. Robust Stability Analysis of DC Microgrids with Constant Power Loads. IEEE Trans Power Syst 2018;33(1):851–60.

[6] Xu Q, Zhang C, Wen C, Wang P. A Novel Composite Nonlinear Controller for Stabilization of Constant Power Load in DC Microgrid. IEEE Trans Smart Grid 2017. https://doi.org/10.1109/TSG.2017.2751755. 1–1.

[7] Khooban Mohammad Hassan, Vafamand Navid, Niknam Taher, Dragicevic Tomislav, Blaabjerg Frede. Model-predictive control based on Takagi-Sugeno fuzzy model for electrical vehicles delayed model. IET Elect Power Appl 2017;11(5):918–34.

[8] Hossain E, Perez R, Padmanaban S, Siano P. Investigation on the development of a sliding mode controller for constant power loads in microgrids. Energies 2017;10 (8):1086–109.

[9] Zeng J, Zhang Z, Qiao W. An interconnection and damping assignment passivity-based controller for a dc–dc boost converter with a constant power load. IEEE Trans Ind Appl 2014;50(4):2314–22.

[10] Zhou J, Wen C. Adaptive backstepping control of uncertain systems: Non smooth nonlinearities, interactions or time-variations. Springer; 2008.

[11] Bechlioulis CP, Rovithakis GA. Robust adaptive control of feedback linearizable MIMO nonlinear systems with prescribed performance. IEEE Trans Autom Control 2008;53(9):2090–9.

[12] Mardani Mohammad Mehdi, Vafamand Navid, Khooban Mohammad Hassan, Dragicevic Tomislav, Blaabjerg Frede. Design of quadratic D-stable fuzzy controller for DC microgrids with multiple CPLs. IEEE Trans Ind Electron 2019;66(6): 4805–12. https://doi.org/10.1109/TIE.2018.2851971.

[13] Herrera L, Zhang W, Wang J. Stability analysis and controller design of DC microgrids with constant power loads. IEEE Trans Smart Grid 2017;8(2):881–8.

[14] Gao F, et al. Comparative stability analysis of droop control approaches in voltage-source-converter-based DC microgrids. IEEE Trans Power Electron 2017;32(3): 2395–415.

[15] Tahim APN, Pagano DJ, Lenz E, Stramosk V. Modeling and stability analysis of islanded DC microgrids under droop control. IEEE Trans Power Electron 2015;30 (8):4597–607.

[16] Aseem K, Selva Kumar S. A novel controller for isolated solar photovoltaic system with super conducting magnetic energy storage and fault ride through capability. Int J Eng Adv Technol 2019;9(1):4344–52.

[17] Jayapriya M, Yadav Shashank, Ram Aravind R, Sathvik S, Lekshmi RR, Selva Kumar S. Implementation of Fuzzy Based Frequency Stabilization Control Strategy in Raspberry Pi for a Wind Powered Microgrid. Procedia Comput Sci 2017;115: 151–8.

[18] Marx D, Magne P, Nahid-Mobarakeh B, Pierfederici S, Davat B. Large Signal Stability Analysis Tools in DC Power Systems with Constant Power Loads and

Variable Power Loads—A Review. IEEE Trans Power Electron 2012;27(4): 1773–87.

[19] Magne P, Nahid-Mobarakeh B, Pierfederici S. General active global stabilization of multiloads DC-power networks. IEEE Trans Power Electron 2012;27(4):1788–98.

[20] Matallana Luis G, Blanco Aníbal M, Alberto Bandoni J. Estimation of domains of attraction: A global optimization approach. Math Comput Model 2010;52:574–85.

[21] Loop B, Sudhoff S, Zak S, Zivi E. Estimating regions of asymptotic stability of power electronics systems using genetic algorithms. IEEE Trans Control Syst Technol 2010;18(5):1011–22.

[22] Nguang S, Shi P. Robust H∞ output feedback control design for fuzzy dynamic systems with quadratic D stability constraints: An LMI approach. Inf Sci 2006;176 (15):2161–91.

[23] Wen J, Nguang SK, Shi P, Nasiri A. Robust H∞ control of discrete-time non-homogenous Markovian jump systems via multistep Lyapunov function approach. IEEE Trans Syst Man Cybernet Syst 2017;47(7):1439–50.

[24] Xie Y, Wen J, Nguang SK, Peng L. Stability, l2-gain and robust H∞ control for switched systems via N-step ahead Lyapunov function approach. IEEE Access 2017; 5(1):26400–8.

[25] Coutinho DF, Trofino A, Fu M. Nonlinear H-infinity Control: an LMI Approach. IFAC15th Triennial World Congress, Barcelona, Spain. 2002.

[26] Fulwani DK, Singh S. Mitigation of Negative Impedance Instabilities in DC Distribution Systems - A Sliding Mode Control Approach. Berlin, Germany: Springer; 2016.

[27] Agarwal A, Deekshitha K, Singh S, Fulwani D. Sliding mode control of a bidirectional dc/dc converter with constant power load. In: Proc. IEEE 1st Int. Conf. DC Microgrids; 2015. p. 287–92.

[28] Saravana Kumar R, Jain A. Design of complementary sliding mode control for variable speed wind turbine. In: ICPES 2018, 8626924; 2018. p. 171–5.

[29] Rajesh R, Kaimal MR. Design of an Adaptive Fuzzy Logic Controller Using MATLAB. MATLAB India Millennium Conference, Bangalore. 2000.

[30] Krishna Karthik P, Anand R. Energy Trading in Microgrids using Block Chain Technology. In: Proceedings of the International Conference on Intelligent Computing and Control Systems, ICICCS 2020; 2020. p. 884–8. 9121050.

[31] Tungal RV, Anand R, Ramprabhakar J. Effective control of three power source dc micro grid using Smart meter. In: Proceedings of the International Conference on Trends in Electronics and Informatics, ICOEI 2019; 2019. p. 797–802.